مجلة الدراسات التربوية والعلمية - كلية التربية - الجامعة العراقية
العدد الخامس والعشرون - المجلد الأول - علوم الفيزياء - آذار 2025 م
doi.org/10.52866/esj.2025.01.25.16

The impact of film thickness on the structural, optical, and electrical characteristics of SnO2 thin films produced using the thermal spraying method

Manar. A. Saleh[1, a] , Zuheer. N. Majeed[2, b]
[1]College of Education for Pure Sciences, Department of Physics, University of Tikrit, Iraq
[2]College of Education for Women, Department of Physics, University of Kirkuk, Iraq
[a)] ma230083pep@st.tu.edu.iq / [b)] zuheernaji@uokirkuk.edu.iq

Abstract :

The objective of this study is to investigate the augmentation of the layer count in SnO2 thin films. Films were created on glass substrates using thermal spraying with different numbers of sputters (10, 20, 30, 40, and 50). Based on the X-ray diffraction (XRD) pattern, the films show a tetracrystalline structure, with the (110) direction displayed at the highest intensity. The data show the generation of samples with crystal diameters ranging from 60 to 120 nm. Through the use of FESEM imaging, it is shown that the nanoparticles underwent a shape transformation, moving from a spherical shape to an agglomerate-like structure in response to changes in thickness, and this resulted in an increase in optical absorption and a decrease in the optical band gap width from 3.93 eV to 3.83 eV. By manipulating the bias voltage and light intensity, it was shown that the photocurrent showed exponential growth, indicating a Schottky-like behavior in the current-voltage (IV) characteristics.

Keywords: SnO2, Thin film, spraying method, characteristics of SnO2, film thickness.

دراسة تأثير زيادة طبقات غشاء SnO2 على الخصائص التركيبية والضوئية والكهربائية المرسبة بطريقة الرش الكيميائي الحراري

منار عبدالله صالح[1] , أ.د زهير ناجي مجيد[2]
كلية التربية للعلوم الصرفة ، قسم الفيزياء , جامعة تكريت , العراق[1]
كلية التربية للبنات ، قسم الفيزياء , جامعة كركوك, العراق[2]

مستخلص:

تدرس هذه الورقة البحثية تأثير زيادة عدد الطبقات أغشية أوكسيد القصدير ، رسبت الأغشية على قواعد زجاجية باستخدام تقنية الرش الكيميائي الحراري، مع ترسيب عدد من الطبقات كل طبقة بعدد رشات مختلفة تبدأ (10، 20، 30، 40، 50) رشة على التوالي. وفقًا لشكل حيود الأشعة السينية (XRD)، تظهر الأغشية بنية رباعية البلورات، حيث يمتلك الاتجاه (110) وهو يعتبر الاتجاهية المفضلة لنمو للاغشية والاعلى شدة . تبين صور و نتائج FESEM عينات بأقطار بلورية تتراوح من 60 إلى 120 نانومتر، لوحظ أن الجسيمات النانوية تخضع لتحولات في الشكل مع تغيرات عند زيادة عدد الطبقات، من الشكل الكروي إلى الهيكل الكروي المتكتل العشوائي ، هذه الزيادة في سمك الغشاء الرقيق تؤدي إلى زيادة امتصاص الضوء وتقليل الفجوة الضوئية ، حيث يتراوح عرض فجوة الطاقة البصرية بين 3.93eV الى 3.83eV. من خلال نتائج جهد الانحياز الامامي والعكسي للتيار- فولتية في حالة الظلام و الضوء، أظهرت النتائج أن التيار الكهروضوئي ينمو بشكل أسي للانحيازين مما يشير إلى أن خصائص تيار-فولتية تُظهر سلوكًا مشابهًا لسلوك شوتكي.

الكلمات المفتاحية: SnO2، الغشاء الرقيق، طرق الترسيب الكيميائي، خصائص SnO2، سمك الغشاء.

1. Introduction

Nano-sized semiconductor metal oxides (MOs) have received much attention due to their interesting electrical and optical properties [1],[2]. Tin dioxide (SnO2), also known as stannous oxide, is a transition metal oxide that has been widely studied and used. Tin oxide, or tin dioxide (SnO2), has a remarkable straight bandgap, making it highly transparent in the visible spectrum. In addition, this compound has chemical and mechanical stability, is environmentally friendly, and has a low level of electrical resistance [3]-[6]. Therefore, SnO2 is used in solar cells, gas sensors, and biosensors [7]-[9]. SnO2, one of the prominent metal oxide semiconductors, is widely used as a gas-sensing material due to its very favorable surfaces for gas adsorption, both physically and chemically [10]. These sensors are very important and play a vital role in the fields of industrial processing, environmental protection, and medical treatment. However, there are additional hurdles that need to be resolved to effectively employ these sensors in different applications. Current efforts are focused on conducting comprehensive research to improve the selectivity, sensitivity, and stability of sensors. Current research is focused on several areas, including the integration of different additives [11], the production of multilayer films [12], the construction of an electronic nose using network recognition algorithms [13], and the application of innovative techniques for the production of sensor films [14]. Recently, there has been an increasing focus on SnO2-based thin-film sensors composed of nanoparticles and nanostructures. The reason for this is that these films show exceptional characteristics, such as small size, high sensitivity, strong stability, fast reaction, and fast recovery. Historically, several conventional techniques have been used to manufacture gas-sensing films. Techniques mentioned include thermochemical spraying, screen printing, physical and chemical vapor deposition (PVD and CVP), dip coating, and gel-based spin coating [15]. However, these methods fail to meet all the criteria necessary to create sensors of exceptional quality. Developing electronics presents a great difficulty in terms of depositing films with complex designs or integrating many gas

detection films on a single chip. This approach has great potential in transferring trace amounts of material and creating pre-defined patterns, giving it an advantage over traditional deposition methods [16]. Spray pyrolysis is a promising technology for material production. Thermal chemical spraying technology is widely used and frequently used. Spray pyrolysis has attracted great interest in the world of materials and device preparation due to its many benefits. The benefits of this technology include the ability to process materials without the need for a vacuum, the ability to perform high-throughput combinatorial chemistry, the ability to process materials at low temperatures, cost-effectiveness, and minimal material waste [14]-[17]. The application of thermal breakdown as a means of producing various functional films, such as thin-film transistors (TFT), has been studied [18]. The research aims to determine the extent of the effect of increasing the number of layers on the membranes and to know the electrical behavior of these membranes.

2. Experimental methods

The fabrication was performed for thin films of tin dioxide on a glass substrate. To begin, glass slides were cleaned ultrasonically for 10 min using a mixture of distilled water and ethanol. Pure SnO2 solution was prepared using aqueous tin chloride SnCl4. 2H2O has the following specifications: molecular weight = 225.63 g/mol, purity = 99.9%, color = white crystals that dissolve quickly in deionized water. Aqueous tin chloride was prepared with molarity (0.1 mol/L) and volume (100 mL). Amounts of 2.4 grams of aqueous tin chloride were dissolved to the desired concentration in 100 M of nonionic water. Then mix the solution using a magnetic mixer for (5-10 minutes). minute. After dissolving the entire substance, the solution is then placed in the tank of the spray device, and the solution is sprayed onto the heated base at a temperature of 300 degrees Celsius for several different sprays (10, 30, 50). This temperature was obtained experimentally in batches over specific time periods. There was a spraying period of 15 seconds and a pause of 60 seconds, to ensure that the temperature of the substrates after spraying returned to its temperature before spraying, which decreased

due to the cooling resulting from the flow spraying. When the deposition process in the previous steps is completed, the glass substrates are then left on the surface of the heater after turning it off until they cool without trying to lift them, to avoid breaking the film when trying to lift it suddenly from the surface of the heater as a result of the temperature difference (rapid cooling).

3. Results and discussion

3.1 Structure and Morphological Properties

Figure 1 displays the X-ray diffraction (XRD) patterns of tin dioxide films that were deposited to glass substrates using different numbers of sprays. The generated films showed a polycrystalline structure and a tetragonal phase, with a diffraction angle of 26.40° and a preferred direction of 110. The diffraction angles of two additional peaks, (101) and (211), were determined to be 33.21° and 51.41°, respectively, and these angles fluctuated slightly. When the number of deposition layers increases. This finding is substantiated by data provided on JCPDS Card No. 00-024-1342 and 01-077-0452. As shown in the figure, three crystalline directions (110), (101), and (211) grew, and the direction (110) was dominant at different numbers of sprays. It is noted that the peaks were low in intensity, not moderate, and regular in shape. The reason is the lack of the number of deposition or crystalline irregularity, which causes some dislocations in the crystal and the breaking of atomic bonds. As the number of layers rises, the magnitude of the peaks intensifies. These findings align with previous studies conducted by other researchers [19]-[21]. The crystal size can be determined using the Debye-Scherer equation, which is expressed as

$$D = k\chi\beta\cos\theta \text{----------} (1)$$

The shape factor, represented by the variable k, has a value of 0.94 in this specific context. The symbol β represents the full width at half maximum, while the diffraction peak angle is called Θ. The X-ray source emits radiation with a wavelength of 0.15=0.15405 nm. It was found that the diameters of the crystals ranged from 60 to 120 nanometers. The data shown in Table 1 demonstrates that there was a noticeable rise in the average crystal size as the number of layers grew from 10 to 50. The number of layers has a direct

impact on both the crystal structure and the size of the nanoparticles. The data indicates a positive correlation between the number of layers and the average crystal size. This implies that as the number of layers, or the amount of material deposited, grows, the average crystal size also increases. The number of layers directly affects all crystal properties. In line with other research [22], [23], our research indicates that there was growth in crystal size when the number of layers was raised from 10 - 50.

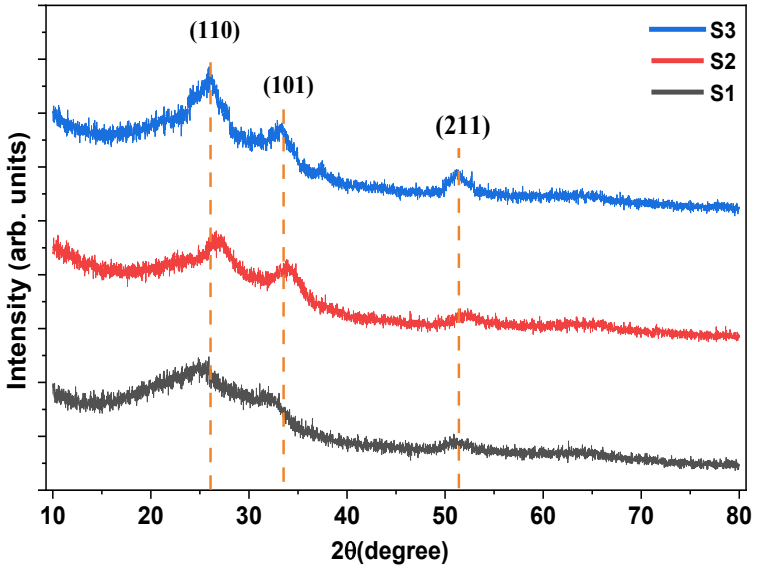

Figure 1: XRD patterns of SnO2- **S1**10-) :Sprinkles), **S2**30-) :Sprinkles), and **S3**50-) :Sprinkles)

Table 1: Characterize the structural properties of the SnO2 thin films formed at various Sprinkles values.: **S1** (10-Sprinkles), **S2** (30-Sprinkles), and **S3** (40-Sprinkles).

Sample	Pos. [°2Th.]	Postcard. [°2Th.]	FWHM [°2Th.]	d-spacing [Å]	d-spacing card [Å]	Rel. Int. [%]	D(nm)	(hlk)
S1	26.4011	26.1884	0.0708	3.14262	3.4	18.88	115.68	110
	33.2119	33.5357	0.0708	2.29753	2.67	14.92	29.36	101
	51.4761	51.5943	0.1417	1.7753	1.77	22.14	62.46	211
S3	26.1577	26.1884	0.2362	3.06277	3.4	53.41	34.66	110
	33.285	33.5357	0.0945	2.61557	2.67	13.59	88.07	101
	51.4179	51.5943	0.144	1.97964	1.77	21.16	61.45	211
S5	26.8436	26.1884	0.3779	3.32132	3.4	28.12	21.69	110
	32.9965	33.5357	0.0708	2.00758	2.67	8	117.46	101
	51.8868	51.5943	0.0708	1.82807	1.77	17.02	125.24	211

3.2. Morphology characterization of SnO2

Figure 2 depicts photographs of tin dioxide samples created by thermal spraying methods. Images were acquired using FESEM, which stands for field emission scanning electron microscopy. The number of sprays (film layers) has a significant influence on both the size and structure of SnO2 nanoparticles, making it a critical factor in their formation. The agglomerated particles showed several distinct shapes. Particles with an average diameter of 30 nm showed a spherical shape and after 10 sprays, the particle size expanded to 60 nm and turned into an oval shape. When the number of sprays increased to 30, the particle size showed a significant decrease to 26 nm at the number of sprays 50, and the structure took the appearance of spheres. Small nanoparticles. Increasing the number of sprays led to the agglomeration process, as shown in SEM images Figure 2: S3 [24].

Figure 3 displays the cross-sectional FESEM picture. The SnO2 films were found to have a thickness of around 72 nm. As the number of spits rises, the material's thickness increases to 174 nm at 30 spits and continues to increase. Spit 30 times. The wavelength is around 1350 nm when using 50 sprays.

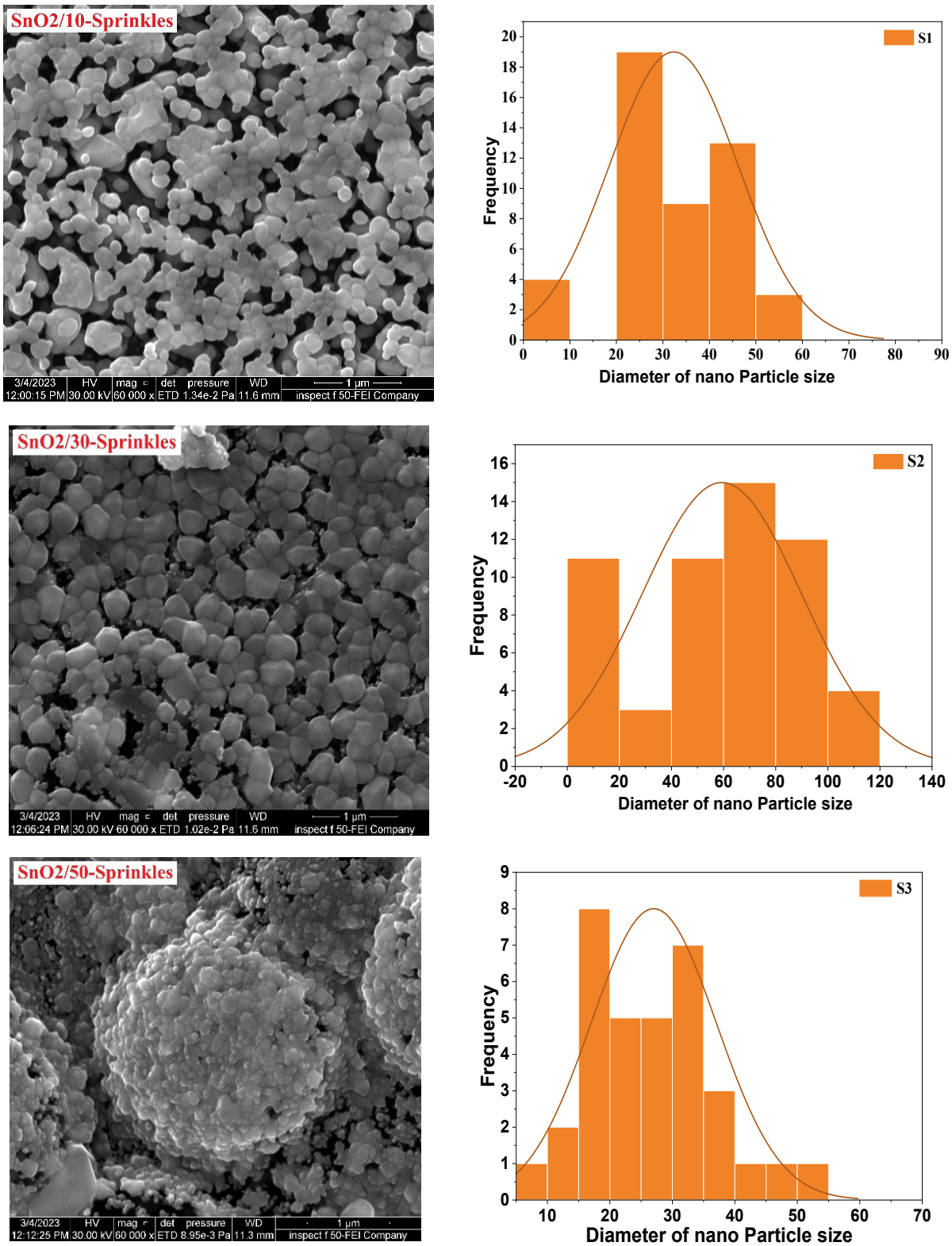

Figure 2: FESEM images of SnO2 at S110-) :Sprinkles), S230-) :Sprinkles), and S350-) :Sprinkles).

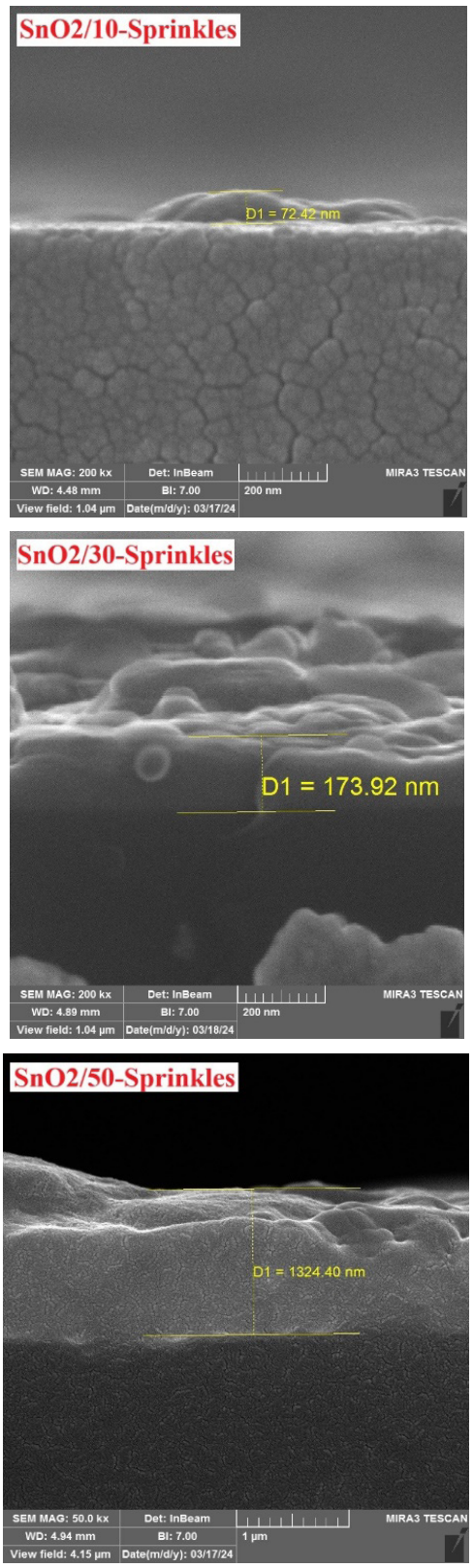

Figure 3: Cross-sectional FESEM image for SnO_2 films at different Sprinkles.

4. Optical properties

Optical absorbance is a critical factor in the operation of many optoelectronic devices, such as solar cells and photodetectors. Figure 4 shows the absorbance spectra, absorption coefficient, and optical energy gap of tin dioxide thin films at many layers (10, 30, and 50). The absorbency level exceeds when the number of sprays increases within the visual range. The curves often exhibit a high level of symmetry due to the even distribution of the film throughout the substrate. The increase in absorbance due to increased film thickness occurs when film thickness levels increase [25].

In Figure 4, the connection was used to elongate the curve between (hv) and $(\alpha hv)^2$ to calculate the optical energy gap of the tin dioxide layer.

$$\propto hv = A(hv - E_g)^{1/2} \text{-------}(2)$$

The absorption coefficient is represented by the symbol (∝), whereas (A) is a fixed numerical value. Using the Tauc formula, we determined the optical band gap values of S1, S2, and S3 to be 3.93, 3.90, and 3.83 eV, respectively. Consistent with prior research, our

investigation produced similar findings [18], [19]. The samples exhibit a reduced optical energy gap in comparison to tin dioxide [26]. The improvement of the photocatalytic efficiency of these samples can mostly be attributed to the reduction of the energy gap at increasing crystalline levels. Materials with a limited range of energy levels between the valence and conduction bands are well suited to act as visible light photocatalysts since they can effectively absorb light at longer wavelengths [27].

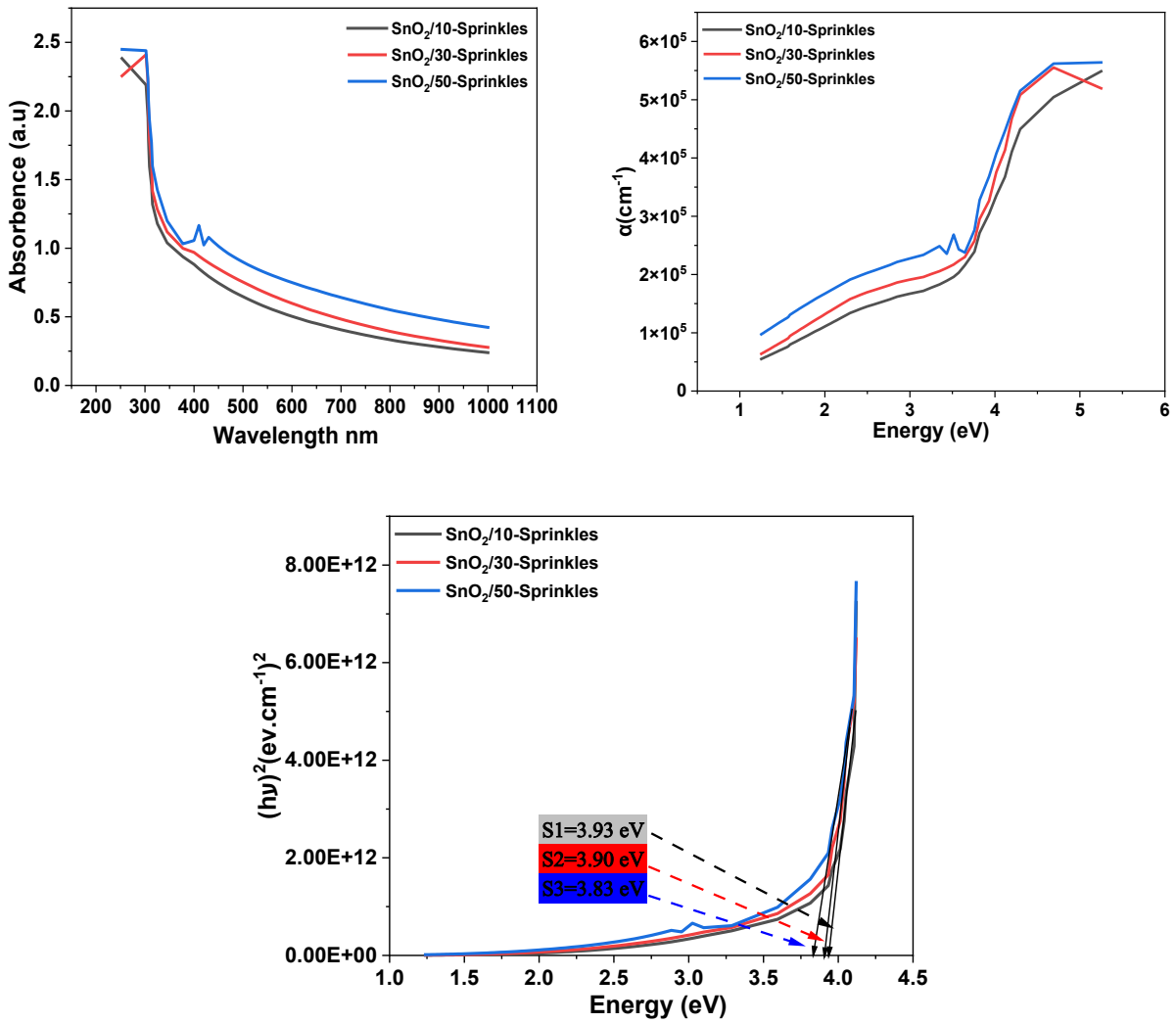

Figure 4: Absorbance, absorption coefficient, and optical energy gap of SnO2 films at **S1**: (10-Sprinkles), **S2**: (30-Sprinkles), and **S3**: (50-Sprinkles).

5. Current-voltage characteristics

The IV property is essential for many interferometric techniques. Measurements of electrical properties were performed on tin dioxide coatings on glass substrates for different number of layers (10, 30, 50) sprays under light and dark conditions. We accomplished this by regularly adjusting the direct current (DC) voltage, ranging from +1V to -1V. The film surface was illuminated using a Philips halogen lamp with a power density of 104.986 mW/cm², at a distance of 20 cm. The input and output were connected by placing aluminum electrodes on the film surface. Voltage and current were measured with a Keithley 2400C. Figure 5 shows the characteristics of the relationship between current and voltage under limited lighting conditions. Recombination currents occur in the high voltage region, which is characterized by a high abundance of minority and majority carriers and a low internal carrier concentration. The majority-carrying dark current is pushed forward by the recombination current. The samples show a slight increase in recombination current within the low voltage range. The transition from the valence band to the conduction band is a plausible explanation and is supported by a viable hypothesis. Due to the overwhelming effect of diffusion current, the current shows exponential growth with increasing voltage. The I-V characteristics of samples S1 and S2 show almost linear and symmetric behavior, indicating the presence of ohmic or subohmic conductors. [28]. This phenomenon arises when aluminum infiltrates the oxide nanostructure, facilitating the movement of electrons through the oxide rather than through the nanostructure itself. All manufactured devices exhibit Schottky behavior in film contact. The graphs show a direct relationship between current voltage and forward bias. The current increased due to the separation of electron-hole pairs and enlargement of the depletion region due to higher reverse bias voltage. Light photons generate an unintended photocurrent. As a result, there is an increasing number of light-generated charge carriers in both the diffusion carrier region and the depletion carrier region [29]. The ability of the device to generate charge carriers in response to light, even in small

amounts, is verified by the slight increase in current observed when it is illuminated [30].

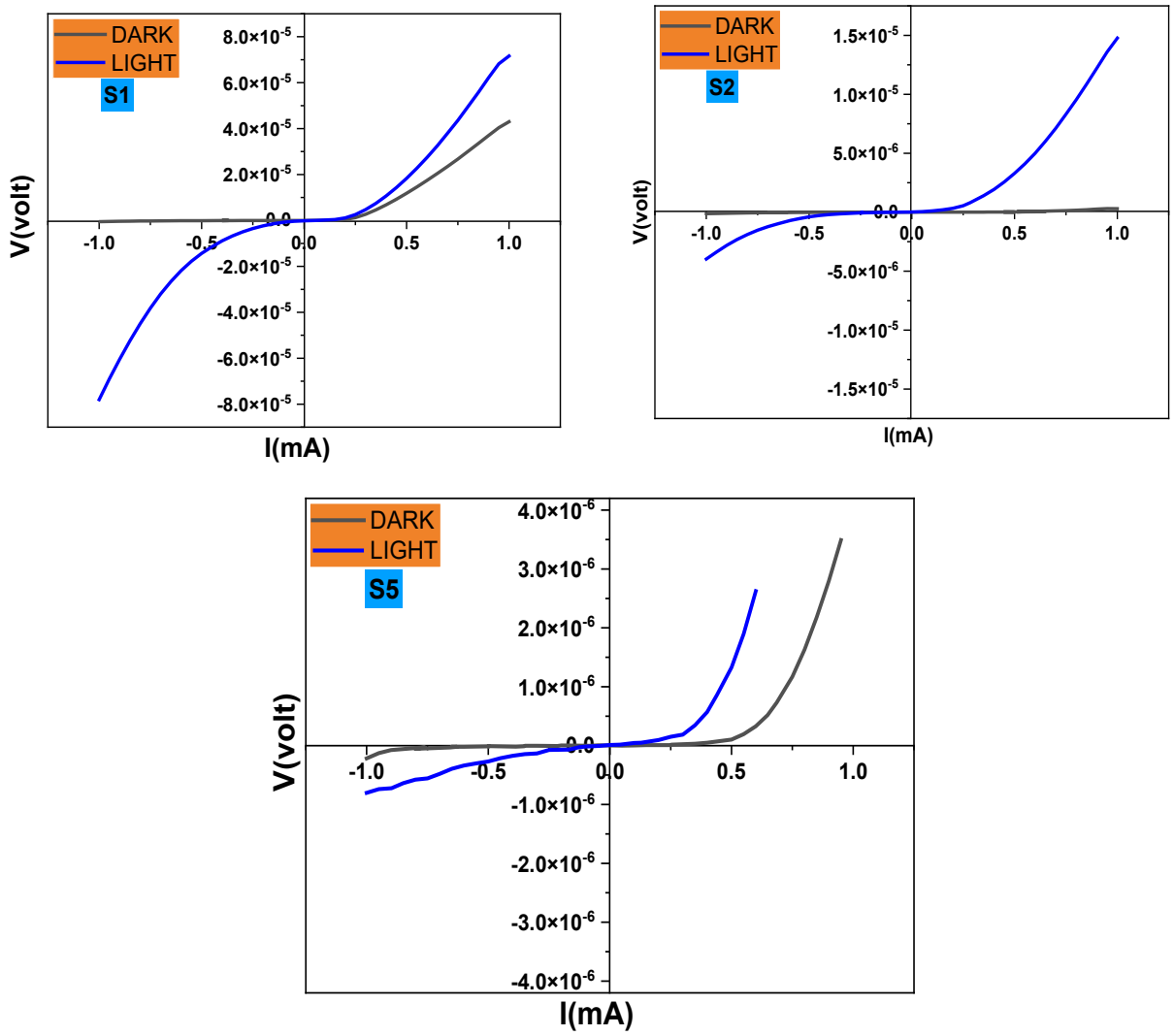

Figure 5: I-V characteristics of the SnO2 films at **S1**: (10-Sprinkles), **S2**: (30-Sprinkles), and **S3**: (50-Sprinkles).

Conclusion

The films underwent hydrothermal treatment to produce nanostructured thin sheets of SnO2. XRD measurements demonstrated the feasibility of manipulating the crystal size by increasing the number of layers. The morphology of the nanoparticles showed variations according to increases in layer number levels, as demonstrated by

images obtained using field emission scanning electron microscopy (FE-SEM). SnO2 thin films showed greater absorption of visible light at the levels of layers with higher thickness. S1, S2, and S3 are measured to have optical energy gaps of 3.93, 3.90, and 3.83 eV, respectively. The current and voltage are achieved and there is an improvement in the electrical properties when the light is incident.

References

[1] S. Ye and T. Endoh, 'Edge effect in the oxidation of three-dimensional nano-structured silicon', Mater Sci Semicond Process, vol. 93, pp. 266–273, 2019.

[2] I. Koltsov et al., 'Novel photocatalytic nanocomposite made of polymeric carbon nitride and metal oxide nanoparticles', Molecules, vol. 24, no. 5, p. 874, 2019.

[3] J. Barbé et al., 'Amorphous tin oxide as a low-temperature-processed electron-transport layer for organic and hybrid perovskite solar cells', ACS Appl Mater Interfaces, vol. 9, no. 13, pp. 11828–11836, 2017.

[4] B. Jang et al., 'High performance ultrathin SnO 2 thin-film transistors by sol–gel method', IEEE Electron Device Letters, vol. 39, no. 8, pp. 1179–1182, 2018.

[5] A. Abdelkrim, S. Rahmane, O. Abdelouahab, N. Abdelmalek, and G. Brahim, 'Effect of solution concentration on the structural, optical and electrical properties of SnO2 thin films prepared by spray pyrolysis', Optik (Stuttg), vol. 127, no. 5, pp. 2653–2658, 2016.

[6] C. Kim and S. Kim, 'Fabrication of tin oxide thin film transistors by RF magnetron sputtering using Sn/SnO composite target', Adv. Mater, vol. 7, no. 3, pp. 73–77, 2018.

[7] O. Vigil-Galán, D. Jiménez-Olarte, G. Contreras-Puente, and M. Courel, 'SnO2 buffer layer deposition for thin film solar cells with superstrate configuration', Journal of renewable and sustainable energy, vol. 7, no. 1, 2015.

[8] P. G. Choi, N. Izu, N. Shirahata, and Y. Masuda, 'Improvement of sensing properties for SnO2 gas sensor by tuning of exposed crystal face', Sens Actuators B Chem, vol. 296, p. 126655, 2019.

[9] Q. Zhou, L. Yang, G. Wang, and Y.

Yang, 'Acetylcholinesterase biosensor based on SnO2 nanoparticles–carboxylic graphene–nafion modified electrode for detection of pesticides', Biosens Bioelectron, vol. 49, pp. 25–31, 2013.

[10] T. Seiyama, A. Kato, K. Fujiishi, and M. Nagatani, 'A new detector for gaseous components using semiconductive thin films.', Anal Chem, vol. 34, no. 11, pp. 1502–1503, 1962.

[11] S. Shamsudin, M. Yahaya, and M. M. Salleh, 'The effect of dopants on the sensing selectivity of SnO/sub 2/thin films-based gas sensors', in ICONIP'02. Proceedings of the 9th International Conference on Neural Information Processing. Computational Intelligence for the E-Age (IEEE Cat. No. 02EX575), IEEE, 2002, pp. 455–457.

[12] M. Yang and S.-H. Hong, 'Fabrication of ITO/SnO2 two-layer thin films and their gas sensing properties', J Electrochem Soc, vol. 157, no. 11, p. J392, 2010.

[13] C. Wongchoosuk, A. Wisitsoraat, A. Tuantranont, and T. Kerdcharoen, 'Portable electronic nose based on carbon nanotube-SnO2 gas sensors and its application for detection of methanol contamination in whiskeys', Sens Actuators B Chem, vol. 147, no. 2, pp. 392–399, 2010.

[14]K. Sahner and H. L. Tuller, 'Novel deposition techniques for metal oxide: Prospects for gas sensing', J Electroceram, vol. 24, pp. 177–199, 2010.

[15] G. Eranna, B. C. Joshi, D. P. Runthala, and R. P. Gupta, 'Oxide materials for development of integrated gas sensors—a comprehensive review', Critical Reviews in Solid State and Materials Sciences, vol. 29, no. 3–4, pp. 111–188, 2004.

[16] J.-P. Viricelle, B. Rivière, and C. Pijolat, 'Optimization of SnO2 screen-printing inks for gas sensor applications', J Eur Ceram Soc, vol. 25, no. 12, pp. 2137–2140, 2005.

[17] C.-H. Chen et al., 'Ink-Jet Printed Passive Electronic Components: Metal-Insulator-Metal Device', in NIP & Digital Fabrication Conference, Society of Imaging Science and Technology, 2005, pp. 76–78.

[18] J. Li et al., 'Ink-jet printed thin-film transistors with carbon nano-

tube channels shaped in long strips', J Appl Phys, vol. 109, no. 8, 2011.

[19] A. A. Yadav, 'Influence of film thickness on structural, optical, and electrical properties of spray deposited antimony doped SnO2 thin films', Thin Solid Films, vol. 591, pp. 18–24, 2015.

[20] C. A. Billur, G. Şahin, E. Güneri, B. Saatçi, and M. Ç. Soylu, 'The effect of films thickness on structural and optical properties of amorphous Sn2O thin films deposited by ink jet printing method', J Mol Struct, vol. 1219, p. 128577, 2020.

[21] H. S. Wasly, A. El-Sadek, S. Elnobi, and A. A. Abuelwafa, 'Morphological, structural, and optical properties of flexible Tin Oxide (II) thin film via thermal evaporation technique', The European Physical Journal Plus, vol. 137, no. 1, pp. 1–10, 2022.

[22] G. Kiruthiga, K. S. Rajni, N. Geethanjali, T. Raguram, E. Nandhakumar, and N. Senthilkumar, 'SnO2: Investigation of optical, structural, and electrical properties of transparent conductive oxide thin films prepared by nebulized spray pyrolysis for photovoltaic applications', Inorg Chem Commun, vol. 145, p. 109968, 2022.

[23] E. Turan, M. Kul, and S. Akın, 'Structural and optical investigation of spray-deposited SnO2 thin films', Journal of Materials Science: Materials in Electronics, vol. 33, no. 19, pp. 15689–15703, 2022.

[24] A. Pramothkumar, N. Senthilkumar, R. M. Jenila, M. Durairaj, T. C. S. Girisun, and I. V. Potheher, 'A study on the electrical, magnetic and optical limiting behaviour of Pure and Cd-Fe co-doped CuO NPs', J Alloys Compd, vol. 878, p. 160332, 2021.

[25] R. L. Orimi and M. Maghouli, 'Optical characterization of SnO2 nanostructure thin films, annealed at different temperatures', Optik (Stuttg), vol. 127, no. 1, pp. 263–266, 2016.

[26] S. Sagadevan and J. Podder, 'Optical and electrical properties of nanocrystalline SnO 2 thin films synthesized by chemical bath deposition method', Soft Nanoscience Letters, vol. 5, no. 04, pp. 55–64, 2015.

[27] A. Paliwal, A. Sharma, M. Tomar, and V. Gupta, 'Dielectric properties of SnO2 thin film using SPR technique for gas sensing applications', in Conference Papers in Science, Wiley Online Library, 2014, p. 656120.

[28] T. Çorlu and S. Acar, 'Investigation of Structural, Morphological and Electrical Properties of SnO2 Thin Film Grown by SILAR Method', Gazi Mühendislik Bilimleri Dergisi, vol. 9, no. 1, pp. 93–99, 2023.

[29] S. K. Mishra, R. K. Srivastava, S. G. Prakash, R. S. Yadav, and A. C. Panday, 'Photoluminescence and photoconductive characteristics of hydrothermally synthesized ZnO nanoparticles', Opto-Electronics Review, vol. 18, no. 4, pp. 467–473, 2010.

[30] Y. R. Hathal, I. M. Ibrahim, and M. K. Khalaf, 'Photosensitivity of Nb2O5/Si Thin Films Produced via DC Reactive Sputtering at Different Substrate Temperatures', Iraqi Journal of Applied Physics, vol. 20, no. 2B, pp. 349–356, 2024.